ISSN 1674-1056
http://cpb.iphy.ac.cn
http://iopscience.iop.org/cpb
中国物理 B
Chinese Physics
中国物理
Chinese Physics B

Low-temperature green synthesis of boron carbide using aloe vera

H V SarithaDevi, M S Swapna, G Ambadas, S Sankararaman

Citation: Chin. Phys. B . 2018, 27(10): 107702. **doi:** 10.1088/1674-1056/27/10/107702

Journal homepage: http://cpb.iphy.ac.cn; http://iopscience.iop.org/cpb

What follows is a list of articles you may be interested in

Effect of oxygen content on dielectric characteristics of Cr-doped $LaTiO_x$

Ming Ma(马铭), Yan Chen(陈彦), Yi-Min Cui(崔益民)

Chin. Phys. B . 2018, 27(5): 057702. **doi:** 10.1088/1674-1056/27/5/057702

First-principles study of the structural, electronic, and magnetic properties of double perovskite Sr_2FeReO_6 containing various imperfections

Yan Zhang(张研), Li Duan(段理), Vincent Ji, Ke-Wei Xu(徐可为)

Chin. Phys. B . 2016, 25(5): 058102. **doi:** 10.1088/1674-1056/25/5/058102

Effects of Ni doping on the structural properties and collapse of magnetic ordering in $NdFe_{1-x}Ni_xO_3$ ($0.1 \leq x \leq 0.7$) orthoferrites

I. Ahmad, M. J. Akhtar, M. Siddique

Chin. Phys. B . 2016, 25(2): 028101. **doi:** 10.1088/1674-1056/25/2/028101

Indium-tin oxide films obtained by DC magnetron sputtering for improved Si heterojunction solar cell applications

Gu Jin-Hua, Si Jia-Le, Wang Jiu-Xiu, Feng Ya-Yang, Gao Xiao-Yong, Lu Jing-Xiao

Chin. Phys. B . 2015, 24(11): 117703. **doi:** 10.1088/1674-1056/24/11/117703

Stability and elastic properties of Nb_xC_y compounds

Gao Xu-Peng, Jiang Ye-Hua, Liu Yang-Zhen, Zhou Rong, Feng Jing

Chin. Phys. B . 2014, 23(9): 097704. **doi:** 10.1088/1674-1056/23/9/097704

Low-temperature green synthesis of boron carbide using aloe vera

H V SarithaDevi[1], M S Swapna[1], G Ambadas[2,†], and S Sankararaman[1,‡]

[1] *Department of Optoelectronics and Department of Nanoscience and Nanotechnology, University of Kerala, Kariavattom, Thiruvananthapuram-695581, Kerala, India*
[2] *Government Victoria College, Palakkad, Kerala, India*

(Received 7 June 2018; revised manuscript received 15 July 2018; published online 27 September 2018)

The unique structural and physical properties of boron carbide, which make it suitable for a wide range of applications, demands the development of low-cost and green synthesis method. In the present work, the commonly available leaves of aloe vera are hydrothermally treated to form the carbon precursor for the synthesis of boron carbide. The morphological characterization reveals the porous nature of the precursor turning into a tubular structure upon boron carbide formation. The structural characterization by x-ray diffraction and other spectroscopic techniques such as Fourier transform infrared, Raman, photoluminescence and uv-visible near-infrared spectroscopy confirm the formation of boron carbide. The thermogravimetric analysis of the sample is found to exhibit good thermal stability above 500 °C. When the sample is annealed to 600 °C, boron carbide with phase purity is obtained, which is confirmed through XRD and FTIR analyses. The optical emission properties of the sample are studied through CIE plot and power spectrum. Compared with other natural precursors for boron carbide, the aloe vera is found to give a good yield above 50%.

Keywords: aloe vera, boric acid, boron carbide, hydrothermal method

PACS: 77.84.Bw, 81.05.Je, 81.05.Rm, 81.05.U– **DOI:** 10.1088/1674-1056/27/10/107702

1. Introduction

Carbides, nitrides, and borides have emerged as a class of advanced ceramic material for targeted applications in industries and electronics. The unique structural, physical and optical properties of carbides, such as greater hardness, higher melting point, temperature stability and optical emission, make them important materials in engineering and technology for wear resistant and refractory applications. Carbides are classified on the basis of chemical bonds into saline, covalent, interstitial, and intermediate, where carbon forms compound with elements of lesser electronegativity.[1] Among these carbides, the boron carbide (B_4C), belonging to the class of covalent carbide, shows some interesting semiconducting and optical properties. Boron carbide films are used in making x-ray mirrors and in the moving parts of tools to enhance tool-life and quality of a machined surface. A wide range of industrial applications has been found, such as wear resistant, ceramic armor, corrosion resistant crucibles, abrasive, lens polisher, high-temperature burners, etc.[2,3] The ability of B_4C to generate electromotive force with thermal gradients leads to the space power generation applications.[4] The greater neutron absorption cross-section and high chemical resistance possess wide applications as a neutron absorber and shielding material in nuclear industry, and the non-oxidative property up to high temperature is suitable for thermoelectric applications.[5,6] The attractive properties such as specific stiffness, specific strength, corrosion resistance and low cost make B_4C an important non-oxide ceramic material.[7] The structure of boron carbide shows a 12-atom icosahedron and a linear arrangement of boron and carbon atoms along the diagonal of the unit cell. The variations by changing the ratio between boron and carbon determine the formation of CBC chain and/or CCC chain, leading the boron carbide to change the structure,[8,9] and thus refractory, electronic, and thermal transport properties.

The increased demand of B_4C for the wide range of applications necessitated the development of various techniques for the synthesis. Compared with other several methods of synthesis, such as chemical vapor deposition, plasma enhanced chemical vapor deposition, synthesis from elements, electrostatic pinning, template-based synthesis, etc., the carbothermal reduction method is the industrially adopted one. The main issue associated with the carbothermal reduction method is the use of toxic chemicals, high temperature, costlier equipment and the adverse influence on the ecosystem. In addition to these, mono-morphology and homogeneity impose limitations on its technical applications. To overcome these limitations, techniques with a wide range of precursors were developed.[10] The development of the eco-friendly synthesis of B_4C using natural precursors is well appreciated.

It is well reported that natural fibers with cellulose as basic units can function as an excellent reinforcement material.[11] The thermal decomposition of carbon chain in cellulose enables the addition of semi-metal atoms like boron and the formation of respective carbides. The fact that plants contain cellulose suitable for turning into carbon precursors

†Corresponding author. E-mail: ambadasg69@gmail.com
‡Corresponding author. E-mail: drssraman@gmail.com

© 2018 Chinese Physical Society and IOP Publishing Ltd

makes them the focus of research in green synthesis. Aloe vera (AV) leaves with gel and neutral sugars with 60% of polysaccharides are widely used for medicinal and agricultural applications.[12,13] Cheng *et al.*[14] reported the production of the cellulose nanofibers by using the chemo-mechanical approach through breaking the hydrogen bonds present in the long chains of cellulose fibers. The present work is an attempt to explore the possibility of turning the AV leaves into natural carbon precursor for the synthesis of B_4C.

2. Experiment

Hydrothermal method is a simple physical and chemical conversion technique for breaking down the long chains of multilayered cellulose with the liberation of –OH groups, making it a functional material that can act as a carbon precursor for the synthesis of B_4C.[15] In the present study, the fresh leaves of AV (*aloe indica*) are used as the raw material for preparing carbon precursors by the hydrothermal method. For this, the fresh leaves of aloe vera are initially washed to remove the dirt, cut into small pieces and then heat-treated in an autoclave under a pressure of about 2×10^2 Pa. After the autoclave treatment, the sample is dried in sunlight for 3–4 days. It is then ground and soaked in 0.1-M hydrochloric acid for 3 h to remove the pulp fiber. The fibrous sample is neutralized (pH = 7) by being washed thoroughly with deionized water and then dried in an air oven for 48 hours (this is denoted as K1). A 10-g dried sample, K1, is added to 50-ml methanol to which 2-g sodium borohydride ($NaBH_4$) is added and dried in an air oven for 1 hour. The dried mixture is annealed in a muffle furnace to 270 °C at a rate of 5 °C/min under controlled air flow condition. The sample is then powdered to which boric acid is added in a ratio 2:1 followed by dispersing it in 20-ml methanol-water mixture (in 1:1 ratio). The resulting sample is refluxed by continuously shaking for 2 hours and then dried in an oven at 120 °C for 3–4 hours and is denoted as K2. The ratio of the amount of K1 to K2 is found to be 50%, whose mixture is annealed at 600 °C to remove the carbon impurities, and also to obtain the more-phase pure sample denoted as K3. The ratio of the amount of K1 to K3 is found to be 33%.

The synthesized sample is subjected to various structural, morphological and optical characterizations. The Field emission scanning electron microscope (FESEM- Hitachi Model D3200) is used to understand the morphology. The thermal stability and yield of the sample are studied from thermogravimetric analysis (TGA- Simultaneous Thermal Analyzer (STA 6000, PerkinElmer)). The structural characterization of the sample is conducted by x-ray diffractometer (Brucker d8 advanced diffractometer) with Cu Kα radiation, Fourier transform infrared (FTIR) spectrophotometer (Shimadzu IRAffinity-1 S) in a region of 4000 cm^{-1}–400 cm^{-1} and Raman spectrophotometer (Alpha300RA- AFM & Raman) with an excitation of 532 nm. The bandgap energy of the sample is determined from ultraviolet-visible NIR (UV-Vis NIR) reflectance spectrum (SHIMADZU UV-3600 plus UV-Vis NIR spectrophotometer) and the luminescent property is studied by using Horiba Fluoromax photoluminescence (PL) spectroscopy. From the PL data, the visual response of the human eye to the optical emission is studied through CIE and power spectrum plots.

3. Results and discussion

The sample (K1) obtained by the hydrothermal treatment of AV exhibits a layered porous morphology which is evidenced from the FESEM image shown in Fig. 1(a). The porous nature is obtained by soaking the autoclave-treated AV, and thus removing the non-cellulosic materials.[13] This porous template of carbon can act as the precursor for the synthesis of boron carbide. The reaction of K1 with $NaBH_4$ enhances the chemical reactivity of carbon precursor by providing hydrate ions that act as a good adsorbent of boron. Further treatment of the sample with boric acid induces drastic changes in the morphology of the sample K1. The ribbon-like morphology of the sample K2 is shown in Fig. 1(b).

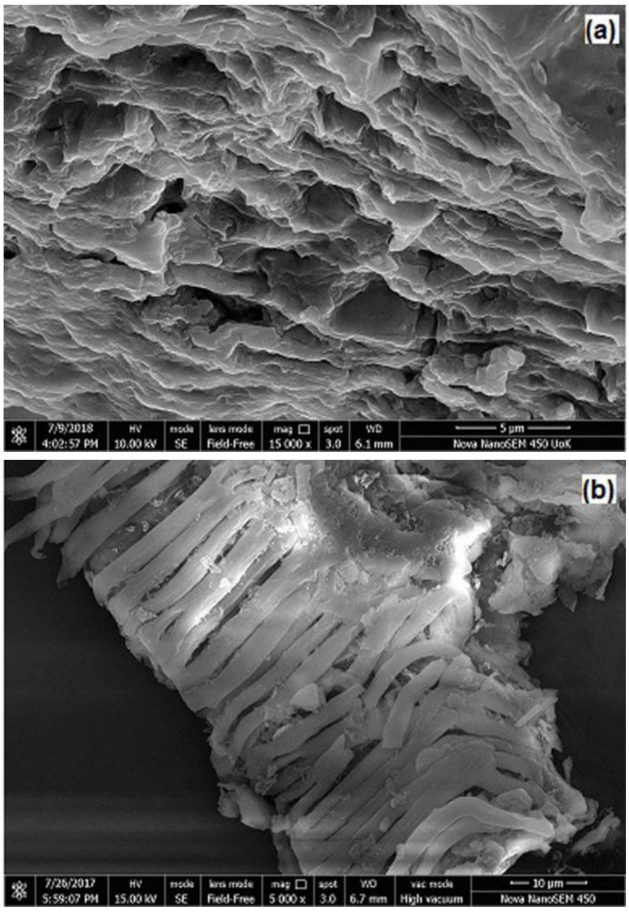


Fig. 1. The FESEM image of samples K1 (a) and K2 (b).

The energy dispersive x-ray spectroscopy (EDS) is a potential tool for estimating the percentage of the elements present in the sample. The EDS of the sample K2 shown in Fig. 2 reveals the percentage composition of boron, carbon, and sodium in the sample. The elemental analysis suggests the formation of boron carbide.

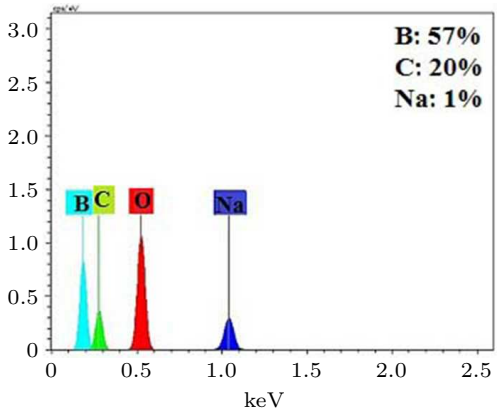


Fig. 2. (color online) Energy dispersive spectrum of sample K2.

The thermal stability and the yield of sample K2 can be understood from the TGA plot shown in Fig. 3. The TGA graph shows three steps around 150 °C, 350 °C, and 500 °C. The slope change around 150 °C arises due to the liberation of water molecules whereas those around 350 °C and 500 °C occur due to the removal of carbon allotropes from the sample. The sample shows good thermal stability above 500 °C and about 55% yield at 900 °C. The precursor aloe vera is found to give a better yield and thermal stability of the synthesized boron carbide than other natural precursors.[16,17] This result is in good agreement with the values obtained during synthesis. For bulk sample (K1) the weight percent yield of K2 and K3 are found to be 50 and 33 respectively.

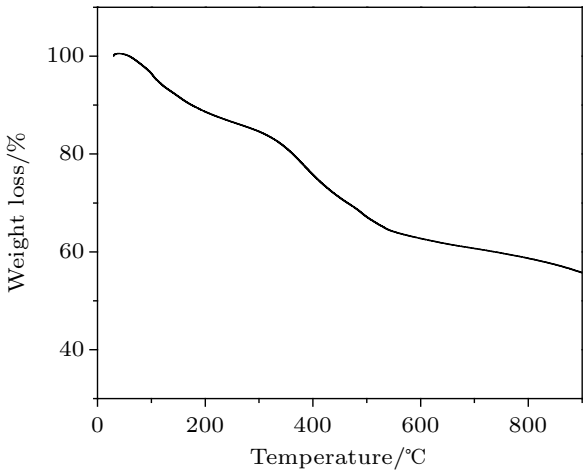


Fig. 3. Thermogram of sample K2.

The FTIR spectroscopy plays a significant role in structure determination. The FTIR spectrum of the synthesized sample K2 is shown in Fig. 4(a). The broad-band around 3400 cm^{-1} is assigned to the C–OH stretching vibration and that at 2360 cm^{-1} and 788 cm^{-1} are attributed to C–H stretching vibrations.[18,19] The narrow bands assigned to B–O stretching vibrations around 1447, 1345, and 924 cm^{-1} [20,21] indicate the incorporation of boron into the sample K2. The absorption bands due to B-C bond at 1638 cm^{-1} and 1258 cm^{-1} are attributed to anti-symmetrical stretching[18] and icosahedral vibrations of boron carbide respectively. In addition, the peaks in the region 550 cm^{-1} to 410 cm^{-1} (shown in the inset of Fig. 4(a)) are assigned to the bending vibrations of the CBC chain.[18,22] The observed characteristic peaks corresponding to the B–C bond and CBC chain indicate the formation of boron carbide in the sample. The FTIR spectrum of the sample K3 (Fig. 4(b)) shows the absence of the peaks corresponding to C–H and B–O stretching vibrations around 2360 cm^{-1} and 924 cm^{-1} respectively indicating the removal of B_2O_3 and carbon impurities. The lowering of the peak intensity around 3400 cm^{-1} indicates the removal of –OH groups. The additional peak of B–B vibration around 822 cm^{-1} [23,24] confirms that the more boron carbide compounds are formed in sample K3.

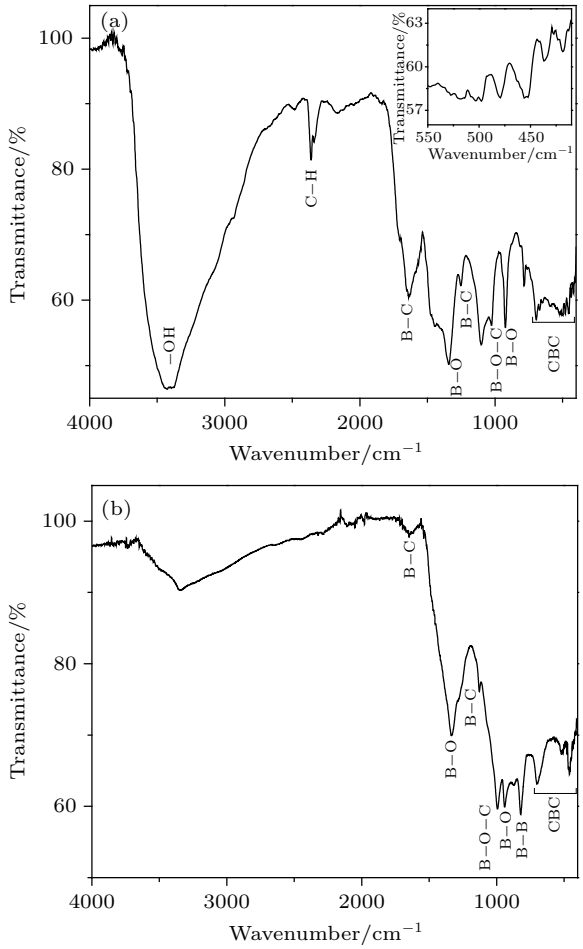


Fig. 4. FTIR spectrum of samples K2 (a) and K3 (b).

Raman spectroscopy is another sensitive tool which provides more information about the structure identification. The

Raman spectrum of the synthesized sample K2 is shown in Fig. 5. The composition of boron carbide contains $B_{11}C$ icosahedra and three-atom inter-icosahedra of CBC chain[8] which are observed in the synthesized sample in two regions (i) 953 cm^{-1}–1198 cm^{-1} and (ii) 227 cm^{-1}–355 cm^{-1} [22,25] respectively. The peak around 1370 cm^{-1} is called the disordered graphite (D–) and a shoulder peak at 1564 cm^{-1} is named graphite (G–) peak,[26] which indicate the presence of carbon in the sample. In addition, the peak at 840 cm^{-1} is assigned to intraicosahedral B–B bond[25] and the characteristic Raman band at 1810 cm^{-1} indicates the presence of amorphous boron carbide.[24]

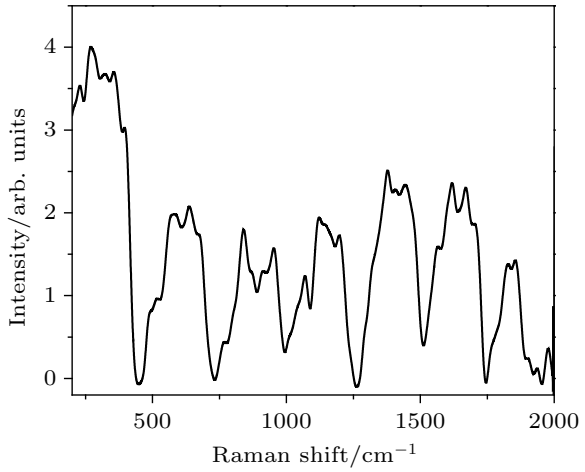


Fig. 5. Raman spectrum of sample K2.

Though the FTIR and Raman spectroscopic analyses indicate the formation of boron carbide, the result can be confirmed only through XRD analysis. The XRD pattern of the samples K1, K2, and K3 are shown in Fig. 6. From Fig. 6(b) it can be seen that the sample K2 shows diffraction peaks around 21°, 31°, 43°, and 69° corresponding to the rhombohedral boron carbide (ICDD file No. 00-019-0178), confirming the formation of B_4C. The characteristic peaks corresponding to orthorhombic boron carbide are also observed at 25°, 29°, and 46° (JCPDS file No. 26-232), indicating the presence of B_8C. In addition, the diffraction peaks around 36° and 39° show the presence of boron oxide and that at 15° corresponds to carbon. When the sample is annealed at 600 °C the formation of more pure B_4C is evident from the twelve characteristic peaks in the XRD pattern shown in Fig. 6(c). The twelve peaks corresponding to the rhombohedral B_4C are at 19°, 20°, 23°, 26°, 31°, 34°, 38°, 40°, 43°, 45°, 51°, and 60° (ICDD file Nos. 00-019-0178 and 00-035-0798). The decrease in the number of peaks corresponding to B_8C, the decrease in peak intensity corresponding to B_2O_3 and the absence of the peak corresponding to carbon in Fig. 6(c) confirm the formation of phase pure boron carbide, B_4C.

The optical property of the sample is studied by UV-Vis NIR reflectance and PL spectroscopic method. The UV-Vis NIR reflectance measurement is obtained between 200 nm–1800 nm and it is shown in Fig. 7. The low energy reflectance

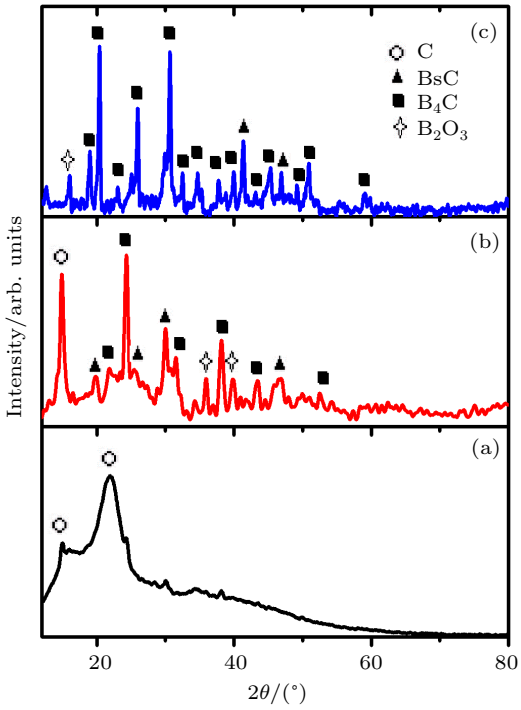


Fig. 6. (color online) XRD pattern of samples (a) K1, (b) K2 and (c) K3.

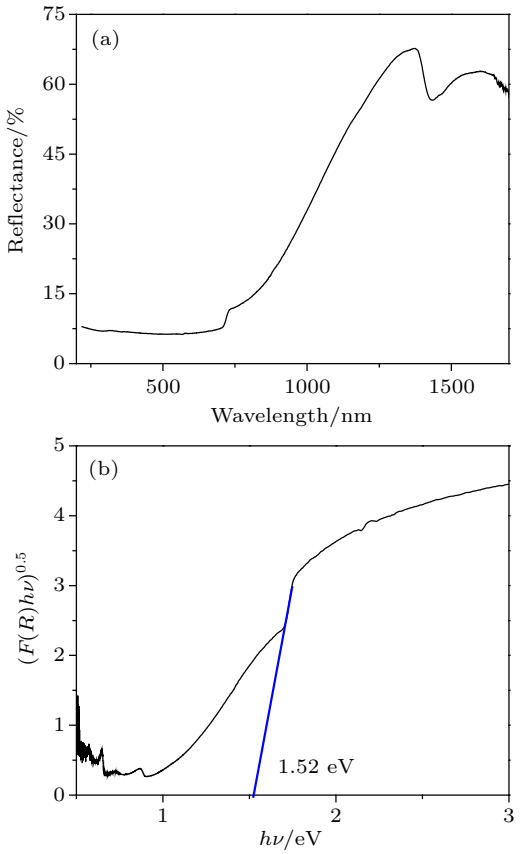


Fig. 7. (color online) (a) UV-Vis NIR reflectance spectrum and (b) Kubelka Munk plot of sample K2.

around 1590 nm is assigned to the stretching of the three-atomic chain and that at 1370 nm indicates the presence of boron in the sample. The bandgap of the synthesized sample, K2, calculated from the reflectance spectrum by the Kubelka Munk method gives 1.52 eV as the indirect bandgap energy. From Fig. 7 it can be seen that the sample shows broad absorption in the region less than 600 nm, indicating the possible π–π^* transition.

From the literature, it can be seen that carbon-based materials show good fluorescence spectra upon photo-excitation. The PL spectroscopy is used to study the electronic structure and properties of the material as a result of the recombination of photo-excited charge carriers. The PL spectrum of the synthesized sample K2 at an excitation of 450 nm is shown in Fig. 8(a). The sample produces emissions, respectively, at wavelengths of 492, 543, 651, 738, and 822 nm, which are corresponding to the optical transitions between the disordered states. The PL spectrum of the annealed sample K3 is shown in Fig. 8(b). Though there is no considerable shift in peak position, the peak intensities turns lower. One can perceive light in a range of 380 nm–750 nm and the color sensitivity can be expressed by using two coordinate CIE system. The emissions from the samples K2 and K3 for the excitation at 450 nm are shown in the chromaticity diagram (Figs. 9(a) and 9(b)) with CIE coordinates (0.38, 0.5) and (0.26, 0.40) respectively. The CIE plots show a shift in the coordinates from yellowish-green to the bluish-white region when the sample becomes purer in phase. How the absorbed optical energy is distributed over the fluorescence spectrum can be understood from the power spectrum shown in Figs. 9(c) and 9(d) of K2 and K3 respectively.

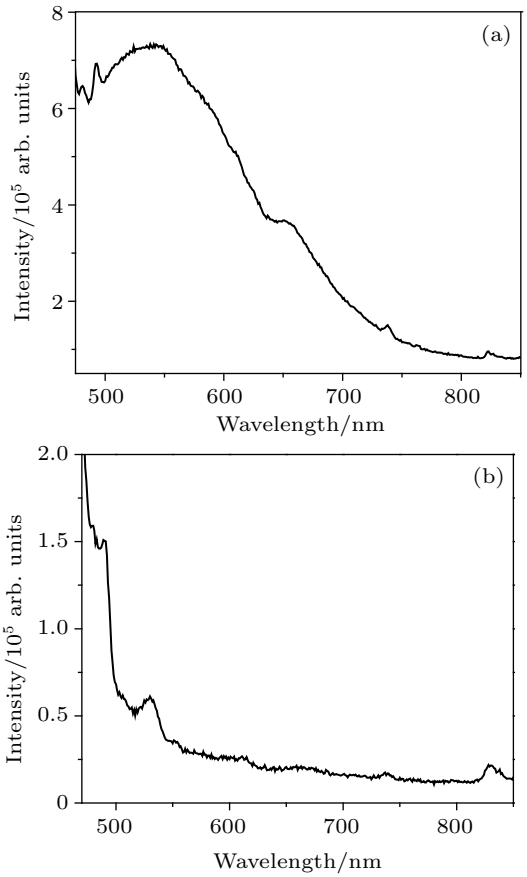


Fig. 8. PL spectra of samples (a) K2 and (b) K3.

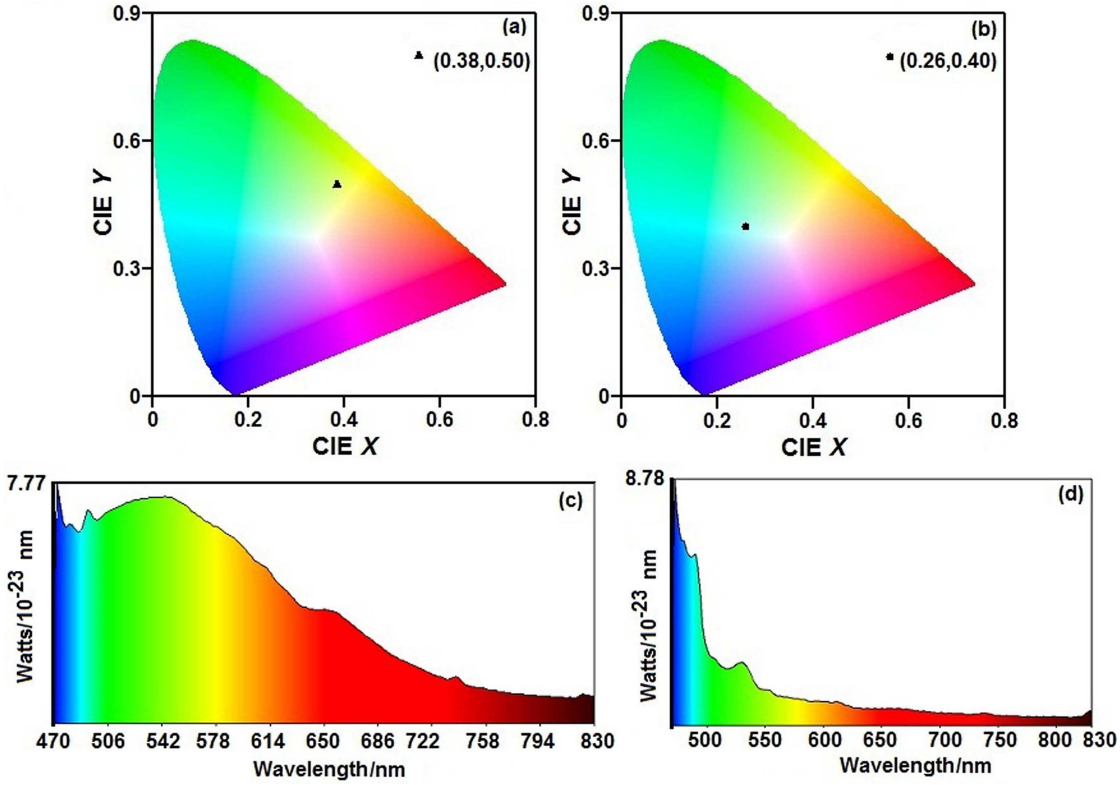


Fig. 9. (color online) CIE plots of samples (a) K2 and (b) K3, and power spectra of samples (c) K2 and (d) K3.

4. Conclusions

In the present work, described is a low-cost, eco-friendly synthesis of boron carbide by using the natural carbon source, aloe vera. The bulk synthesis of boron carbide by the present hydrothermal method with aloe vera rind as carbon precursor is found to give a better result. The morphological and elemental characterizations are performed by FESEM and EDS. The structural characterizations by FTIR, Raman and XRD techniques reveal the formation of boron carbide. The FTIR spectrum and XRD pattern of the sample annealed at 600 °C is found to give a more phase pure B_4C with the elimination of carbon. The TGA reveals the good thermal stability for the sample above 500 °C with a yield 55% whereas the annealing of bulk samples to obtain K2 and K3 are found to give a yield of 50% and 33% respectively. The UV-Vis-NIR spectrum indicates the presence of CBC chain, which confirms the formation of boron carbide with an indirect bandgap energy of 1.52 eV. The fluorescence analysis is carried out to understand the optical emission by the samples, and the distributions of optical power over the spectrum are depicted through the CIE and power spectrum plots. The precursor aloe vera is found to give a better yield above 50% of boron carbide than other natural precursors.

Acknowledgment

One of the authors (Amar P Misra) acknowledges support from UGC-SAP (DRS, Phase III) with Sanction order No. F.510/3/DRS-III/2015(SAPI), and UGC-MRP with F. No. 43-539/2014 (SR) and FD Diary No. 3668.

References

[1] Kosolopova T Y 1971 *Carbides: Properties, Production and Applications* (NewYork: Plenum Press)
[2] Pierson H O 1996 *Handbook of refractory carbides and nitrides: Properties, Characteristics, Processing and Applications* (USA: Noyes Publications)
[3] Avciata O, Ergun C, Erden I, Ustundag C, Yilmaz S and Cihangir S 2008 *ICC*2 *Proceedings on Global Roadmap for Ceramics*, Verona
[4] Mondal S and Banthia A K 2005 *J. Eur. Ceram. Soc.* **25** 287
[5] Sun J, Ling H, Pan W J, Xu N, Ying Z F, Shen W D and Wu J D 2004 *TriBiology Letters* **17** 99
[6] Sariyer D, Kucer R and Kucer N 2015 *Procedia Soc. Behavioral Sci.* **195** 1752
[7] Kakiage M, Tahara N, Yanase I and Kobayashi H 2011 *Mater. Lett.* **65** 1839
[8] Tallant D R, Aselage T L, Campbell A N and Emin D 1989 *Phys. Rev. B* **40** 5649
[9] Ektarawong A, Simak S I and Alling B 2016 *Phys. Rev. B* **94** 054104
[10] Yanase I, Ogawara R and Kobayashi H 2009 *Mater. Lett.* **63** 91
[11] Swapna M S, Saritha Devi H V, Riya S, Ambadas G and Sankararaman S 2017 *Mater. Res. Express* **4** 125602
[12] Hamman J H 2008 *Molecules* **13** 1599
[13] Karnan M, Subramani K, Sudhan N, Ilayaraja N and Sathish M 2016 *Appl. Mater. Interfaces* **8** 35191
[14] Cheng S, Panthapulakkal S, Sain M and Asiri A 2014 *J. Appl. Polym. Sci.* **131** 40592
[15] Pinkowska H, Wolak P and Zlocinska A 2012 *Chem. Eng. J.* **187** 410
[16] Saritha Devi H V, Swapna M S, Vimal R, Ambadas G and Sankararaman S 2018 *Mater. Res. Express* **5** 015603
[17] Saritha Devi H V, Swapna M S, Ambadas G and Sankararaman S 2018 *Appl. Phys. A* **124** 297
[18] Romanos J, Beckner M, Stalla D, Tekeei A, Suppes G, Jalisatgi S, Lee M, Hawthorne F, Robrtson J D, Firlej L, Kuchta B, Wexler C, Yu P and Pfeifer P 2013 *Carbon* **54** 208
[19] Fan M, Dai D and Huang B 2012 *Fourier transform infrared spectroscopy for natural fibers*, Mohammed S ed., Chapter 3 in Fourier Transform-Materials Analysis, INTECH 45
[20] Mortensen M W, Sorensen P G, Bjorkdahl O, Jensen M R, Gundersen H J G and Bjornholm T 2006 *Appl. Radiat. Isot.* **64** 315
[21] Zhuang D W, Dai H B and Wang P 2013 *RSC Adv.* **3** 23810
[22] Domnich V, Reynaud S, Haber R A and Chhowalla M 2011 *J. Am. Ceram. Soc.* **94** 3605
[23] Zorzi J E, Perottoni C A and Jornada J A H D 2005 *Mater. Lett.* **59** 2932
[24] Wang J Z, He Y, Xie Z F, Chen C L, Yang Q B, Zhang C L, Wang B Y, Zhan Y Q and Zhao T H 2017 *Polym. Adv. Technol.* **29** 757
[25] Ahmed M Z, El-Sheikh M, Ewais M M, Abd-Allah A and Sayed A 2017 *JMEPEG* **26** 1444
[26] Yan X Q, Li W J, Goto T and Chen M W 2006 *Appl. Phy. Lett.* **88** 131905